

**Direct spectroscopic evidence for completely filled Cu 3d shell in BaCu<sub>2</sub>As<sub>2</sub> and  $\alpha$ -BaCu<sub>2</sub>Sb<sub>2</sub>**S. F. Wu,<sup>1</sup> P. Richard,<sup>1,2,\*</sup> A. van Roekeghem,<sup>1,3</sup> S. M. Nie,<sup>1</sup> H. Miao,<sup>1</sup> N. Xu,<sup>4</sup> T. Qian,<sup>1</sup> B. Saparov,<sup>5,†</sup> Z. Fang,<sup>1,2</sup> S. Biermann,<sup>3,6,7</sup> Athena S. Sefat,<sup>5</sup> and H. Ding<sup>1,2,‡</sup><sup>1</sup>Beijing National Laboratory for Condensed Matter Physics, and Institute of Physics, Chinese Academy of Sciences, Beijing 100190, China<sup>2</sup>Collaborative Innovation Center of Quantum Matter, Beijing, China<sup>3</sup>Centre de Physique Théorique, Ecole Polytechnique, CNRS-UMR7644, 91128 Palaiseau, France<sup>4</sup>Swiss Light Source, Paul Scherrer Institut, CH-5232 Villigen PSI, Switzerland<sup>5</sup>Materials Science and Technology Division, Oak Ridge National Laboratory, 1 Bethel Valley Road, Oak Ridge, Tennessee 37831, USA<sup>6</sup>Collège de France, 11 place Marcelin Berthelot, 75005 Paris, France<sup>7</sup>European Theoretical Synchrotron Facility (ETSF), Europe

(Received 1 April 2015; published 8 June 2015)

We use angle-resolved photoemission spectroscopy to extract the band dispersion and the Fermi surface of BaCu<sub>2</sub>As<sub>2</sub> and  $\alpha$ -BaCu<sub>2</sub>Sb<sub>2</sub>. While the Cu 3d bands in both materials are located around 3.5 eV below the Fermi level, the low-energy photoemission intensity mainly comes from As 4p states, suggesting a completely filled Cu 3d shell. The splitting of the As 3d core levels and the lack of pronounced three-dimensionality in the measured band structure of BaCu<sub>2</sub>As<sub>2</sub> indicate a surface state likely induced by the cleavage of this material in the collapsed tetragonal phase, which is consistent with our observation of a Cu<sup>+1</sup> oxidation state. However, the observation of Cu states at similar energy in  $\alpha$ -BaCu<sub>2</sub>Sb<sub>2</sub> without the pnictide-pnictide interlayer bonding characteristic of the collapsed tetragonal phase suggests that the short interlayer distance in BaCu<sub>2</sub>As<sub>2</sub> follows from the stability of the Cu<sup>+1</sup> rather than the other way around. Our results confirm the prediction that BaCu<sub>2</sub>As<sub>2</sub> is an *sp* metal with weak electronic correlations.

DOI: [10.1103/PhysRevB.91.235109](https://doi.org/10.1103/PhysRevB.91.235109)

PACS number(s): 74.70.Xa, 74.25.Jb, 79.60.-i, 71.20.-b

Even today, the cuprate superconductors constitute the family of unconventional superconductors exhibiting the highest critical temperatures. The parent compounds of the cuprates are strongly correlated materials with Cu in the 3d<sup>9</sup> configuration (Cu<sup>2+</sup>) bridged by oxygen. Chalcogen and pnictogen atoms also serve as bridges in the layered Fe-based superconductors, for which typical electronic band renormalization factors of 2–5 are usually found [1]. Naively, one would expect that a Cu-based material crystallizing in the same crystal structure as a Fe-based superconductor should also show strong electronic correlations and possible superconductivity, thus motivating the study of such compounds. Not only is superconductivity not observed in BaCu<sub>2</sub>As<sub>2</sub> [2], this material has been predicted to be an *sp* metal with a filled 3d shell [3]. Unfortunately, there is still no spectroscopic evidence supporting this scenario.

Here we report an angle-resolved photoemission spectroscopy study of the electronic band dispersion and the Fermi surface of BaCu<sub>2</sub>As<sub>2</sub> and  $\alpha$ -BaCu<sub>2</sub>Sb<sub>2</sub>. Our photon energy-dependent study reveals that the Cu 3d states are located around 3.5 eV below the Fermi level ( $E_F$ ), whereas the intensity around  $E_F$  is mainly derived from As 4p states. The experimental Fermi surfaces of both materials are very similar and qualitatively consistent with those of  $\alpha$ -BaCu<sub>2</sub>Sb<sub>2</sub> derived from generalized gradient approximation (GGA) calculations. Except for the lack of three-dimensionality in BaCu<sub>2</sub>As<sub>2</sub> associated with a surface state following the cleavage of samples in the collapsed tetragonal phase, the experimental

band dispersions are also consistent with nonrenormalized GGA calculations, suggesting the absence of strong electronic correlations. Our angle-resolved photoemission spectroscopy (ARPES) results indicate that BaCu<sub>2</sub>As<sub>2</sub> and  $\alpha$ -BaCu<sub>2</sub>Sb<sub>2</sub> have a fully filled Cu 3d shell and that the stability of this electronic configuration favors the collapsed tetragonal phase of BaCu<sub>2</sub>As<sub>2</sub>.

Large single crystals of BaCu<sub>2</sub>As<sub>2</sub> and  $\alpha$ -BaCu<sub>2</sub>Sb<sub>2</sub> were grown by the self-flux method [2]. ARPES measurements were performed at the PGM and APPLE-PGM beamlines of the Synchrotron Radiation Center (Wisconsin) equipped with a VG-Scienta R4000 analyzer and a SES 200 analyzer, respectively. The energy and angular resolutions for the angle-resolved data were set at 10–30 meV and 0.2°, respectively. The samples were cleaved *in situ* and measured at 20 K in a working vacuum better than  $5 \times 10^{-11}$  Torr. In the following, we label the momentum values with respect to the 1 Cu/unit cell Brillouin zone and use  $c' = c/2$  as the distance between two Cu planes. Raman scattering measurements were performed using argon-krypton laser lines in a back-scattering micro-Raman configuration with a triple-grating spectrometer (Horiba Jobin Yvon T64000) equipped with a nitrogen-cooled CCD camera. In this manuscript, we define  $x$  and  $y$  as the directions along the  $a$  or  $b$  axes, oriented 45° from the Cu-Cu bounds, while  $x'$  and  $y'$  are defined as the Cu-Cu directions. We performed first-principles calculations of the electronic band structure by using the full-potential linearized-augmented plane-wave (FP-LAPW) method implemented in the WIEN2K package for the crystal structures of BaCu<sub>2</sub>As<sub>2</sub> and  $\alpha$ -BaCu<sub>2</sub>Sb<sub>2</sub> [2]. The exchange-correlation potential was treated using the GGA based on the Perdew-Burke-Ernzerhof (PBE) approach [4].

The crystal structures of BaCu<sub>2</sub>As<sub>2</sub> and  $\alpha$ -BaCu<sub>2</sub>Sb<sub>2</sub> are closely related, as illustrated by the insets of Figs. 1(a) and 1(b).

\*p.richard@iphy.ac.cn

†Present address: Department of Mechanical Engineering and Materials Science, Duke University, Durham, NC 27708, USA.

‡dingh@iphy.ac.cn

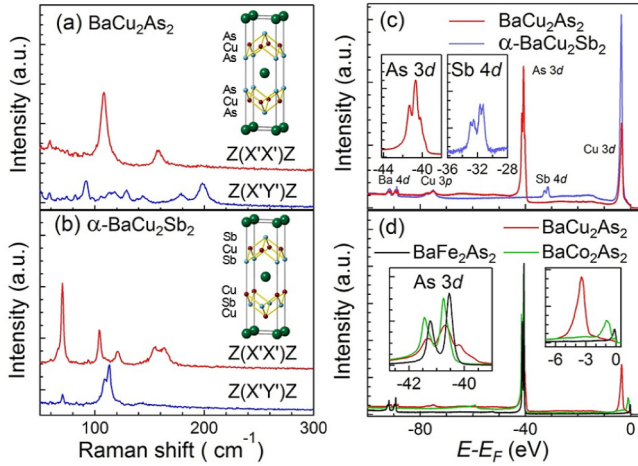


FIG. 1. (Color online) (a) and (b) Polarized *ab* plane Raman spectra of  $\text{BaCu}_2\text{As}_2$  and  $\alpha\text{-BaCu}_2\text{Sb}_2$  at 294 K. Insets: corresponding crystal structures. (c) Core levels of  $\text{BaCu}_2\text{As}_2$  and  $\alpha\text{-BaCu}_2\text{Sb}_2$  recorded at 180 eV. The inset zooms on the As 3*d* and Sb 4*d* core levels of  $\text{BaCu}_2\text{As}_2$  and  $\alpha\text{-BaCu}_2\text{Sb}_2$ , respectively. (d) Comparisons of the core levels of  $\text{BaM}_2\text{As}_2$  for  $M = \text{Fe}, \text{Co},$  and  $\text{Cu}$ , recorded at 180 eV. The insets show the zooms on the As 3*d* core levels and the valence band.

While  $\text{BaCu}_2\text{As}_2$  has the same crystal structure as  $\text{BaFe}_2\text{As}_2$ , described by the space group  $D_{4h}^{17} (I4/mmm)$ ,  $\alpha\text{-BaCu}_2\text{Sb}_2$ , characterized by the space group  $D_{4h}^7 (P4/nmm)$ , has the relative positions of the Sb and Cu atoms exchanged in two successive layers. To confirm that our samples of  $\text{BaCu}_2\text{As}_2$  and  $\alpha\text{-BaCu}_2\text{Sb}_2$  have different crystal structures, we recorded Raman spectra at room temperature with incident and scattered light polarized in the *ab* plane. Our analysis predicts four Raman active modes in  $\text{BaCu}_2\text{As}_2$  ( $A_{1g} + B_{1g} + 2E_g$ ) and nine in  $\alpha\text{-BaCu}_2\text{Sb}_2$  ( $3A_{1g} + 2B_{1g} + 4E_g$ ). While the in-plane polarization used does not allow us to detect  $E_g$  modes, the  $A_{1g}$  (related to the vibration of the pnictogens along the *c* axis) and  $B_{1g}$  (related to the vibration of Cu) channels are accessible in the  $z(x'x')\bar{z}$  and  $z(x'y')\bar{z}$  configurations, respectively. The experimental results for  $\text{BaCu}_2\text{As}_2$  and  $\alpha\text{-BaCu}_2\text{Sb}_2$  are shown in Figs. 1(a) and 1(b), respectively. We observe an  $A_{1g}$  mode at  $108.9 \text{ cm}^{-1}$  and a  $B_{1g}$  mode at  $198.2 \text{ cm}^{-1}$  in  $\text{BaCu}_2\text{As}_2$ , whereas three  $A_{1g}$  modes at  $70.4 \text{ cm}^{-1}$ ,  $104 \text{ cm}^{-1}$ , and  $121.4 \text{ cm}^{-1}$  and two  $B_{1g}$  modes at  $108.7 \text{ cm}^{-1}$  and  $113.4 \text{ cm}^{-1}$  are detected in  $\alpha\text{-BaCu}_2\text{Sb}_2$ . Although additional weak and unidentified peaks are also detected, the spectra of our  $\text{BaCu}_2\text{As}_2$  and  $\alpha\text{-BaCu}_2\text{Sb}_2$  samples are clearly different, thus proving that they correspond to different crystal phases.

We then confirm the elemental composition of our samples by showing the core-level spectra of  $\text{BaCu}_2\text{As}_2$  and  $\alpha\text{-BaCu}_2\text{Sb}_2$  in Fig. 1(c). In both materials we detect the Ba 4*d* and Cu 3*p* core levels around 90 and 75 eV of binding energy ( $E_B$ ), respectively. As expected, the spectrum of  $\text{BaCu}_2\text{As}_2$  exhibits additional peaks at around 41 eV corresponding to the As 3*d* states that do not appear in the spectrum of  $\alpha\text{-BaCu}_2\text{Sb}_2$ . However, four features instead of two are observed, suggesting a surface state similar to the one reported previously for the  $\text{EuFe}_2\text{As}_{2-x}\text{P}_x$  system [5]. The spectra of  $\alpha\text{-BaCu}_2\text{Sb}_2$  exhibits four peaks around  $E_B = 32 \text{ eV}$  assigned to the Sb

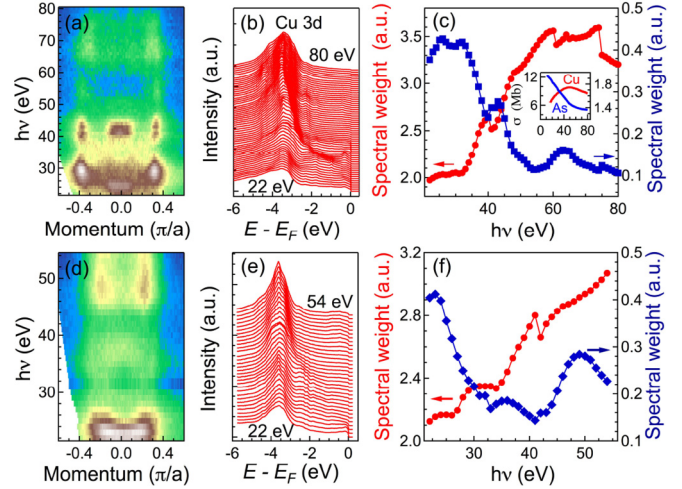


FIG. 2. (Color online) (a) Photon energy ( $h\nu$ ) dependence of the ARPES intensity (integration within  $E_F \pm 10 \text{ meV}$ ) in  $\text{BaCu}_2\text{As}_2$  recorded at 20 K along  $\Gamma\text{-}M$ . (b) Corresponding EDC curves. (c)  $h\nu$  dependence of the spectral weight in  $\text{BaCu}_2\text{As}_2$  integrated within the  $[-4, -3] \text{ eV}$  (red) and  $[-1, 0] \text{ eV}$  (blue) ranges. The inset shows the Cu 3*d* and As 4*p* photoemission cross sections. (d)–(f) Same as (a)–(c) but for  $\alpha\text{-BaCu}_2\text{Sb}_2$ .

4*d* electronic states. In this case, though, the existence of four Sb peaks does not indicate the presence of a surface state, since the crystal structure of  $\alpha\text{-BaCu}_2\text{Sb}_2$  itself contains two inequivalent Sb sites.

A rigid band shift is the simplest assumption one can make when describing the effect of doping. When considering only the *shape* of the quasiparticle dispersions, this assumption works surprisingly well in the  $(\text{Ba},\text{K})\text{Fe}_2\text{As}_2$  and  $\text{Ba}(\text{Fe},\text{Co})_2\text{As}_2$  systems [6], despite a strong dependence of the strength of correlations and coherence on the filling [7]. It is also still valid when the filling of the 3*d* shell reaches seven electrons in  $\text{BaCo}_2\text{As}_2$  [8]. As illustrated in the left inset of Fig. 1(d) that compares the As 3*d* core levels of  $\text{BaFe}_2\text{As}_2$ ,  $\text{BaCo}_2\text{As}_2$ , and  $\text{BaCu}_2\text{As}_2$ , the As 3*d* core levels in  $\text{BaCo}_2\text{As}_2$  are downshifted in energy compared to their energy position in  $\text{BaFe}_2\text{As}_2$ , indicating an upward shift of the chemical potential. Assuming that the Cu 3*d* shell in  $\text{BaCu}_2\text{As}_2$  contains nine electrons as in the cuprates, a large downshift of the core-level position should be observed. In contrast, the center of gravity of the As 3*d* core levels in  $\text{BaCu}_2\text{As}_2$  is found nearly at the same energy as in  $\text{BaFe}_2\text{As}_2$ . This indicates clearly that the rigid band-shift approximation is no longer valid and that other effects, such as the electronic valency of As, must be considered. A direct corollary is that the valency of the Cu atoms, which have As as ligands, may also be strongly affected.

To check this latter scenario, we performed ARPES measurements of the valence states. In Fig. 2(a) we display the photon energy ( $h\nu$ ) dependence of the ARPES intensity at  $E_F$  recorded along  $\Gamma\text{-}M$  in  $\text{BaCu}_2\text{As}_2$ . Although the intensity is modulated along  $k_z$ , the momentum position of the features observed varies very little with  $h\nu$ , suggesting a quasi-two-dimensional electronic structure. Thus we can tentatively assign the  $h\nu$  values 41 and 36 eV to  $k_z = 0$  and  $k_z = \pi$ , but we cannot unambiguously determine which one

is which. Despite a different crystal structure, very similar results are observed for  $\alpha$ -BaCu<sub>2</sub>Sb<sub>2</sub>, as shown in Fig. 2(d), except that the  $k_z$  values associated with  $h\nu = 36$  and 41 eV are exchanged.

The  $h\nu$  dependence of the normal emission energy distribution curves (EDCs) in BaCu<sub>2</sub>As<sub>2</sub> and  $\alpha$ -BaCu<sub>2</sub>Sb<sub>2</sub> are displayed in Figs. 2(b) and 2(e), respectively. Unlike the ferropnictide materials, for which strong spectral weight associated to the Fe 3*d* states is observed near  $E_F$  [9], BaCu<sub>2</sub>As<sub>2</sub> and  $\alpha$ -BaCu<sub>2</sub>Sb<sub>2</sub> exhibit only very small intensity at  $E_F$ . On the other hand, the Cu-pnictides show a very strong peak around 3.5 eV below  $E_F$ . In Fig. 2(c) we compare the spectral intensity of the normal emission EDCs integrated in the  $[-4, -3]$  eV and  $[-1, 0]$  energy ranges. The  $h\nu$  dependencies of these spectral intensities show different trends, thus indicating that their origin is different. While the spectral intensity in the  $[-4, -3]$  eV range increases with  $h\nu$ , increasing from 22 to about 60 eV and then slowly decreasing, the spectral intensity near  $E_F$  is at its highest at low  $h\nu$  values and drops with increasing  $h\nu$ . Besides additional features, like the small peaks around 41 and 64 eV in the  $[-1, 0]$  energy range that are likely induced by the  $k_z$  effect on the photoemission matrix elements, the intensity of the  $[-4, -3]$  eV and  $[-1, 0]$  eV ranges are qualitatively in reasonable agreement with the photoemission cross sections [10] of the Cu 3*d* and As 4*p* states, respectively, which are reproduced in the inset of Fig. 2(c). A similar observation is made for  $\alpha$ -BaCu<sub>2</sub>Sb<sub>2</sub>, as illustrated by Figs. 2(e)–2(f).

The results discussed above indicate clearly that most of the Cu 3*d* states are located at about 3.5 eV below  $E_F$ . We thus conclude that unlike in the cuprates, the 3*d* shell of Cu is completely filled, an experimental conclusion consistent with a previous prediction based on a local density approximation (LDA) study of BaCu<sub>2</sub>As<sub>2</sub> and SrCu<sub>2</sub>As<sub>2</sub> [3]. Experimentally, a Fermi surface different from that of the ferropnictides, essentially made of pnictogen states, is thus expected. In Figs. 3(a) and 3(b), we compare the Fermi surface intensity maps obtained on BaCu<sub>2</sub>As<sub>2</sub> using  $h\nu = 41$  and 36 eV, respectively. In agreement with the  $h\nu$  dependence of the intensity plot shown in Fig. 2(a) and despite a redistribution of spectral intensity along the Fermi surface, the measured Fermi surfaces for these two sets of data are surprisingly similar, indicating a quasi-two-dimensional electronic structure. This is in sharp contrast with our GGA calculation of the three-dimensional Fermi surface of this material, which is displayed in Fig. 3(c), as well as with the calculated Fermi surface cuts at  $k_z = 0$  and  $k_z = \pi$ , shown in Fig. 3(g). Even more surprising is the strong resemblance between the results recorded on BaCu<sub>2</sub>As<sub>2</sub> and those recorded on  $\alpha$ -BaCu<sub>2</sub>Sb<sub>2</sub>, which are displayed in Figs. 3(d) and 3(e), although the features obtained for  $\alpha$ -BaCu<sub>2</sub>Sb<sub>2</sub> are broader, which we attribute to a bad surface quality due to the difficulty of cleaving this material with strong Cu-Sb interlayer bonding. Unlike BaCu<sub>2</sub>As<sub>2</sub>,  $\alpha$ -BaCu<sub>2</sub>Sb<sub>2</sub> is predicted to have a two-dimensional Fermi surface, as illustrated in Fig. 3(f) and by the Fermi surface cuts at  $k_z = 0$  and  $k_z = \pi$  given in Figs. 3(h) and 3(i), respectively.

In Fig. 4, we display the ARPES curvature [11] intensity plots of BaCu<sub>2</sub>As<sub>2</sub> and  $\alpha$ -BaCu<sub>2</sub>Sb<sub>2</sub> recorded at 20 K along some high-symmetry lines with 41 and 36 eV photons. As mentioned above, the quasi-two-dimensional nature of the

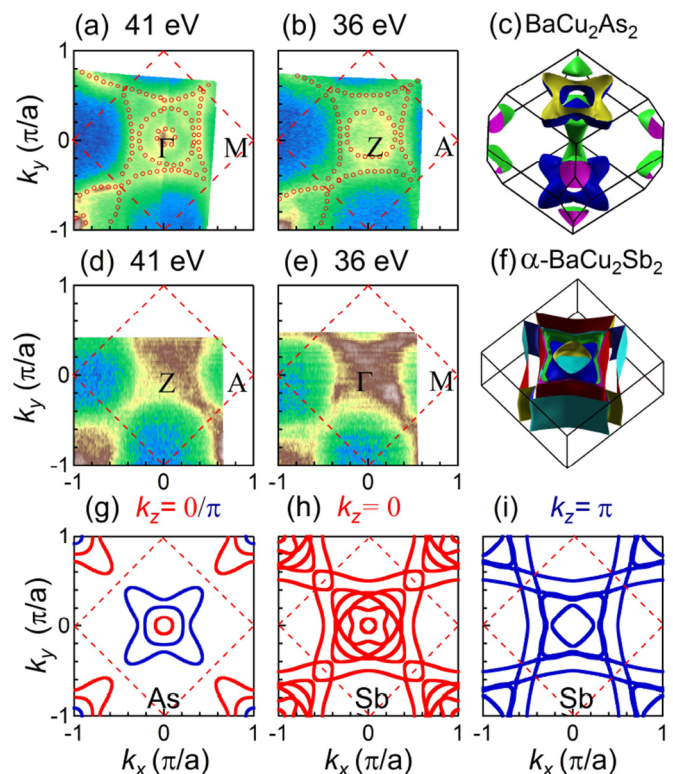


FIG. 3. (Color online) (a), (b) ARPES intensity plot of BaCu<sub>2</sub>As<sub>2</sub> recorded at 20 K ( $\pm 10$  meV integration around  $E_F$ ) with 41 and 36 eV, respectively. The dots are guides for the eye for the Fermi surfaces. (c) Calculated three-dimensional Fermi surface of BaCu<sub>2</sub>As<sub>2</sub>. (d), (e) Same as (a) and (b) but for  $\alpha$ -BaCu<sub>2</sub>Sb<sub>2</sub>. (f) Calculated three-dimensional Fermi surface of  $\alpha$ -BaCu<sub>2</sub>Sb<sub>2</sub>. (g) Calculated GGA Fermi surface of BaCu<sub>2</sub>As<sub>2</sub> at  $k_z = 0$  (red) and  $k_z = \pi$  (blue). (h) Calculated GGA Fermi surface of  $\alpha$ -BaCu<sub>2</sub>Sb<sub>2</sub> at  $k_z = 0$ . (i) Calculated GGA Fermi surface of  $\alpha$ -BaCu<sub>2</sub>Sb<sub>2</sub> at  $k_z = \pi$ .

experimental Fermi surfaces prevents us from identifying unambiguously which one corresponds to  $k_z = 0$  and which one corresponds to  $k_z = \pi$ , but our  $h\nu$  dependence data suggest that the roles are exchanged in BaCu<sub>2</sub>As<sub>2</sub> and  $\alpha$ -BaCu<sub>2</sub>Sb<sub>2</sub>. For these plots we tentatively assume that 41 eV corresponds to  $k_z = 0$  ( $k_z = \pi$ ) in BaCu<sub>2</sub>As<sub>2</sub> ( $\alpha$ -BaCu<sub>2</sub>Sb<sub>2</sub>). Except for a few obvious discrepancies, like the absence of an electron pocket at  $\Gamma$  in the experimental data and the position of the holelike dispersion around  $\Gamma$ , the GGA calculations at  $k_z = 0$  capture well the main features observed experimentally, without any renormalization. A similar comment can be made for  $\alpha$ -BaCu<sub>2</sub>Sb<sub>2</sub>, although in that case the agreement of the experimental data and the GGA predictions for the location of the Cu 3*d* bands is slightly worse.

Given the indications of the presence of a surface state, we have tried to understand the striking resemblance of the measured BaCu<sub>2</sub>As<sub>2</sub> spectral function with the one of  $\alpha$ -BaCu<sub>2</sub>Sb<sub>2</sub> by assuming that the ARPES spectra display a substantial contribution from the surface layer. In BaFe<sub>2</sub>As<sub>2</sub>, a surface relaxation that consists essentially in an elongation of the As height at the surface has been studied in Ref. [12]. The result of such a structural surface relaxation is that the two FeAs layers of the surface unit cell are no longer equivalent,



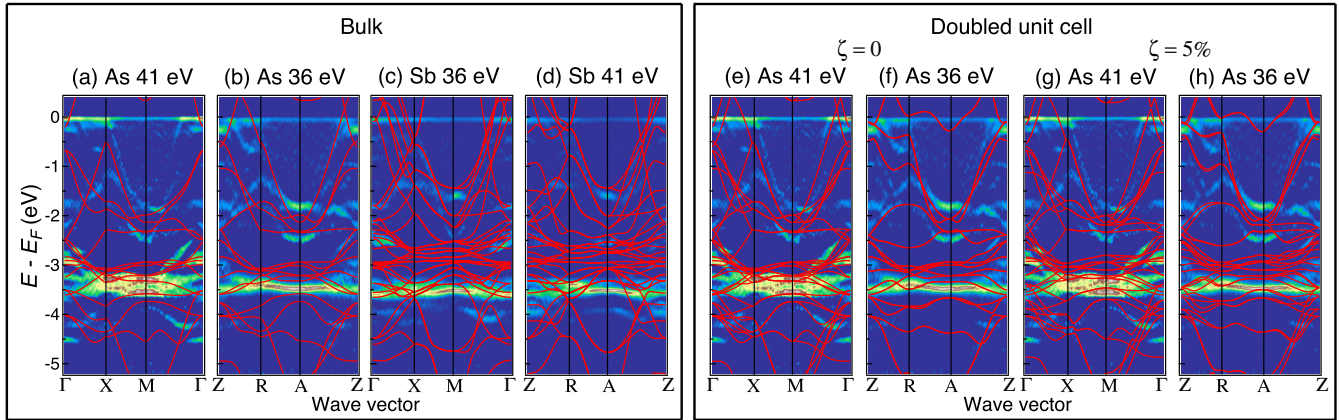


FIG. 4. (Color online) Comparison of unrenormalized GGA calculations (red curves) and curvature intensity plots for the electronic dispersion along high-symmetry lines: (a)  $\text{BaCu}_2\text{As}_2$  at 41 eV, GGA at  $k_z = 0$ ; (b)  $\text{BaCu}_2\text{As}_2$  at 36 eV, GGA at  $k_z = \pi$ ; (c)  $\alpha\text{-BaCu}_2\text{Sb}_2$  at 36 eV, GGA at  $k_z = 0$ ; (d)  $\alpha\text{-BaCu}_2\text{Sb}_2$  at 41 eV, GGA at  $k_z = \pi$ . (e), (f) Same as (a) and (b) but with the calculations done for a hypothetical  $\text{BaCu}_2\text{As}_2$  compound where we have lowered the crystal symmetry as if two consecutive CuAs layers were inequivalent in order to simulate the surface. The relative variation of the As height position with respect to the Cu plane, for the two consecutive As layers  $\zeta$ , is fixed to 0. (g), (h) Same as in (e) and (f) but for the parameter  $\zeta = 5\%$ .

putting the surface crystal structure in the same symmetry group as the bulk of  $\alpha\text{-BaCu}_2\text{Sb}_2$ , namely,  $P4/nmm$ , where two inequivalent layers appear due to the inversion of Cu and Sb. To the best of our knowledge, the precise surface crystal structure of  $\text{BaCu}_2\text{As}_2$  has not been characterized yet, but it seems plausible that the “collapsed” character of this phase rather enhances such a structural distortion at the surface, and it is safe to postulate that a substantial distortion, leaving the two uppermost CuAs surface layers inequivalent, occurs.

Now, we can speculate that chemically, substituting Sb by As does not result in a drastic difference in the spectra, as long as the crystal symmetry is preserved. We have checked this hypothesis by calculating the band structure of a hypothetical  $\text{BaCu}_2\text{As}_2$  compound where we have lowered the crystal symmetry as if the two layers were inequivalent. The resulting bands are overlaid to the experimental data in Figs. 4(e) and 4(f). We also show the band structure that we obtain if we increase the As height by 5% on one of the layers, in Figs. 4(g) and 4(h). One of the consequences of such a doubled unit cell is that the number of bands in the  $k_z = 0$  plane is multiplied by 2 due to folding [Figs. 4(e) and 4(g)], and the dispersion corresponds to a superposition of the bands in the  $k_z = 0$  and  $k_z = \pi$  plane of the  $I4/mmm$  structure [Figs. 4(a) and 4(b)]. In the  $k_z = \pi$  plane of the doubled unit cell, the number of bands is also multiplied by 2, but they are degenerate if the two layers have the same structure [Fig. 4(f)], while a difference appears if we introduce a distortion [Fig. 4(h)]. While the knowledge of the precise surface structure would be needed to obtain quantitative agreement, Figs. 4(e)–4(h) strongly suggest that the similarity of the  $\text{BaCu}_2\text{As}_2$  spectra to the  $\alpha\text{-BaCu}_2\text{Sb}_2$  spectra can indeed be attributed to a lowering of the surface crystal symmetry of the kind we describe.

Finally, we comment on the  $3d^{10}$  configuration of Cu. Singh already pointed out [3] that the much shorter  $c$  parameter in  $\text{BaCu}_2\text{As}_2$  as compared to  $\text{BaNi}_2\text{As}_2$  and  $\text{BaFe}_2\text{As}_2$  is suggestive of different bonding in  $\text{BaCu}_2\text{As}_2$ , which is confirmed by our As  $3d$  core-level spectra. In fact, comparison of the lattice parameters places  $\text{BaCu}_2\text{As}_2$  in the collapsed

tetragonal phase [13], which is associated with a stronger As-As interlayer bonding [14,15]. However, our results suggest that the strong As-As interlayer bonding cannot be the cause of the  $3d^{10}$  configuration of Cu in  $\text{BaCu}_2\text{As}_2$ . Indeed, the  $3d$  Cu states in  $\alpha\text{-BaCu}_2\text{Sb}_2$  are located practically at the same energy as in  $\text{BaCu}_2\text{As}_2$ , despite the absence of Sb-Sb direct interlayer bonding in the former material, thus reinforcing previous arguments by Anand *et al.* based on the resemblance of the physical properties of  $\text{SrCu}_2\text{As}_2$  and  $\alpha\text{-SrCu}_2\text{Sb}_2$  [13]. Interestingly, the Cu dopant states in Cu-substituted  $\text{BaFe}_2\text{As}_2$  are also found around 3–4 eV below  $E_F$  [16,17], suggesting that Cu dopants are already in a +1 oxidation state. This is consistent with the absence of any shift in the Cu  $2p$  core-level spectra as a function of doping [18], as well as with the suppression of magnetic moment and the observation of superconductivity only for a very narrow Cu substitution range [19,20], in contrast to substitution of Fe by Co [21,22] and Ni [23]. However, the clear observation of added electron carriers in  $\text{Ba}(\text{Fe}_{1-x}\text{Cu}_x)_2\text{As}_2$  [19,20] indicates that the Cu substitution is electron doping; nevertheless, suggesting that the local As-As and As-transition metal bondings are strongly affected, a situation that could be stabilized at high substitution levels by the collapsed tetragonal phase. Our findings support the hypothesis [13] that it is the stability of the  $3d^{10}$  configuration of Cu ( $\text{Cu}^{+1}$ ) that favors the collapsed tetragonal phase of  $\text{BaCu}_2\text{As}_2$ , rather than the other way around.

In summary, we have performed angle-resolved photoemission spectroscopy measurements on  $\text{BaCu}_2\text{As}_2$  and  $\alpha\text{-BaCu}_2\text{Sb}_2$  to extract their electronic band dispersions and Fermi surfaces. We found that most of the Cu  $3d$  spectral weight locates around 3–4 eV below  $E_F$ , whereas the intensity around  $E_F$  mainly comes from As  $4p$  bands, suggesting a filled Cu  $3d$  shell. The observation of split As  $3d$  core levels and the absence of pronounced three-dimensionality in the measured electronic structure of  $\text{BaCu}_2\text{As}_2$  is compatible with a surface state emerging from the cleavage of this material in the collapsed tetragonal phase. However, the observation of similar Cu  $3d$  states in  $\alpha\text{-BaCu}_2\text{Sb}_2$  without

pnictide-pnictide interlayer bonding suggests that the stability of the  $\text{Cu}^{+1}$  configuration favors the collapsed tetragonal phase rather than the other way around. Our study indicates that  $\text{BaCu}_2\text{As}_2$  and  $\alpha\text{-BaCu}_2\text{Sb}_2$  are *sp* metals with weak electronic correlations.

We acknowledge W.-L. Zhang for useful discussions. This work was supported by grants from Ministry of Science and Technology of China (No. 2010CB923000, No. 2011CBA001000, No. 2011CBA00102, and No. 2012CB821403) and NSFC (No. 10974175, No. 11004232,

No. 11034011/A0402, No. 11234014, and 11274362) from China, the Cai Yuanpei program, the French ANR via project PNICTIDES, IDRIS/GENCI under Project No. 091393, and the European Research Council under Project No. 617196. This work is based in part on research conducted at the Synchrotron Radiation Center, which was primarily funded by the University of Wisconsin-Madison with supplemental support from facility users and the University of Wisconsin-Milwaukee. The work at ORNL was supported by the Department of Energy, Basic Energy Sciences, Materials Sciences and Engineering Division.

- 
- [1] P. Richard, T. Sato, K. Nakayama, T. Takahashi, and H. Ding, *Rep. Prog. Phys.* **74**, 124512 (2011).
- [2] B. Saparov and A. S. Sefat, *J. Solid State Chem.* **191**, 213 (2012).
- [3] D. J. Singh, *Phys. Rev. B* **79**, 153102 (2009).
- [4] J. P. Perdew, K. Burke, and M. Ernzerhof, *Phys. Rev. Lett.* **77**, 3865 (1996).
- [5] P. Richard, C. Capan, J. Ma, P. Zhang, N. Xu, T. Qian, J. D. Denlinger, G.-F. Chen, A. S. Sefat, Z. Fisk, and H. Ding, *J. Phys.: Condens. Matter* **26**, 035702 (2014).
- [6] M. Neupane, P. Richard, Y.-M. Xu, K. Nakayama, T. Sato, T. Takahashi, A. V. Federov, G. Xu, X. Dai, Z. Fang, Z. Wang, G.-F. Chen, N.-L. Wang, H.-H. Wen, and H. Ding, *Phys. Rev. B* **83**, 094522 (2011).
- [7] P. Werner, M. Casula, T. Miyake, F. Aryasetiawan, A. J. Millis, and S. Biermann, *Nature Phys.* **8**, 331 (2012).
- [8] N. Xu, P. Richard, A. van Roekeghem, P. Zhang, H. Miao, W.-L. Zhang, T. Qian, M. Ferrero, A. S. Sefat, S. Biermann, and H. Ding, *Phys. Rev. X* **3**, 011006 (2013).
- [9] H. Ding, K. Nakayama, P. Richard, S. Souma, T. Sato, T. Takahashi, M. Neupane, Y.-M. Xu, Z.-H. Pan, A. V. Fedorov, Z. Wang, X. Dai, Z. Fang, G. F. Chen, J. L. Luo, and N. L. Wang, *J. Phys.: Condens. Matter* **23**, 135701 (2011).
- [10] J. Yeh and I. Lindau, *At. Data Nucl. Data Tables* **32**, 1 (1985).
- [11] P. Zhang, P. Richard, T. Qian, Y.-M. Xu, X. Dai, and H. Ding, *Rev. Sci. Instrum.* **82**, 043712 (2011).
- [12] V. B. Nascimento, Ang Li, Dilushan R. Jayasundara, Yi Xuan, J. O'Neal, Shuheng Pan, T. Y. Chien, Biao Hu, X. B. He, Guorong Li, A. S. Sefat, M. A. McGuire, B. C. Sales, D. Mandrus, M. H. Pan, Jiandi Zhang, R. Jin, and E. W. Plummer, *Phys. Rev. Lett.* **103**, 076104 (2009).
- [13] V. K. Anand, P. K. Perera, A. Pandey, R. J. Goetsch, A. Kreyssig, and D. C. Johnston, *Phys. Rev. B* **85**, 214523 (2012).
- [14] R. Hoffmann and C. Zheng, *J. Phys. Chem.* **89**, 4175 (1985).
- [15] T. Yildirim, *Phys. Rev. Lett.* **102**, 037003 (2009).
- [16] J. A. McLeod, A. Buling, R. J. Green, T. D. Boyko, N. A. Skorikov, E. Z. Kurmaev, M. Neumann, L. D. Finkelstein, Ni Ni, A. Thaler, S. L. Bud'ko, P. C. Canfield, and A. Moewes, *J. Phys.: Condens. Matter* **24**, 215501 (2012).
- [17] S. Ideta, T. Yoshida, I. Nishi, A. Fujimori, Y. Kotani, K. Ono, Y. Nakashima, S. Yamaichi, T. Sasagawa, M. Nakajima *et al.*, *Phys. Rev. Lett.* **110**, 107007 (2013).
- [18] Y. J. Yan, P. Cheng, J. J. Ying, X. G. Luo, F. Chen, H. Y. Zou, A. F. Wang, G. J. Ye, Z. J. Xiang, J. Q. Ma, and X. H. Chen, *Phys. Rev. B* **87**, 075105 (2013).
- [19] E. D. Mun, S. L. Bud'ko, Ni Ni, A. N. Thaler, and P. C. Canfield, *Phys. Rev. B* **80**, 054517 (2009).
- [20] N. Ni, A. Thaler, J. Q. Yan, A. Kracher, E. Colombier, S. L. Bud'ko, P. C. Canfield, and S. T. Hannahs, *Phys. Rev. B* **82**, 024519 (2010).
- [21] A. S. Sefat, R. Jin, M. A. McGuire, B. C. Sales, D. J. Singh, and D. Mandrus, *Phys. Rev. Lett.* **101**, 117004 (2008).
- [22] N. Ni, M. E. Tillman, J.-Q. Yan, A. Kracher, S. T. Hannahs, S. L. Bud'ko, and P. C. Canfield, *Phys. Rev. B* **78**, 214515 (2008).
- [23] L. J. Li, Y. K. Luo, Q. B. Wang, H. Chen, Z. Ren, Q. Tao, Y. K. Li, X. Lin, M. He, Z. W. Zhu, G. H. Cao, and Z. A. Xu, *New J. Phys.* **11**, 025008 (2009).